

Supporting Information

Surface Activated Carbon Nitride Nanosheets with Optimized Electro-optical Properties for Highly Efficient Photocatalytic Hydrogen Production

Mohammad Ziaur Rahman,^a Jingrun Ran,^a Youhong Tang,^b Mietek Jaroniec^c and Shi Zhang Qiao^a

E-mail: s.qiao@adelaide.edu.au

^a*School of Chemical Engineering, The University of Adelaide, SA 5005, Australia.*

^b*School of Computer Science, Engineering and Mathematics, Flinders University, SA 5001, Australia.*

^c*Department of Chemistry and Biochemistry, Kent State University, Kent, Ohio 44240, USA*

I. Experimental and Calculation Section

A. Synthesis

Synthesis of the bulk CN: Synthesis of bulk CN was carried out through the molecular intercalation of dicyandiamide (DCDA) and thiourea followed by polymerization-polycondensation at moderately high temperature. Molecular derivatives of precursors were prepared by dissolving 3 g of DCDA and 3 g of thiourea in a mixed solution of DI water and ethanol (1:0.5 vol%) under vigorous stirring at 80 °C for 24 h in a water bath followed by drying in an oven at 70 °C overnight. Next, the white intercalated mixture of DCDA and thiourea was transferred to a ceramic boat and calcined at 550 °C (2.3 °C/min ramp) for 4 h in a tube furnace under N₂ flow. After cooling down furnace to room temperature, a light yellowish bulk CN was obtained.

Surface activation of the bulk CN: The as-synthesized bulk CN was transferred into a ceramic crucible and heated in a muffle furnace under aerobic conditions at 550 °C (2.0 °C/min ramp) for 3 h. After cooling down furnace to room temperature, an agglomerated CN was obtained.

Synthesis of NS-CN nanosheets: The surface-activated carbon nitride powder was diluted in DI water and ultra-sonicated for 10 hours in a water bath at room

temperature. The milky-colour solution was then centrifuged at 12,000 rpm for 10 min, washed with DI water two times. Finally, the whitish milky solution was dried in a vacuum oven at 60 °C for 24 hours to obtain NS-CN nanosheet-type powder.

Synthesis of GCN: The reference GCN was also prepared according to the procedure reported elsewhere.¹ In a typical synthesis, 4 g of DCDA were calcined in a tube furnace at 550 °C (2.3 °C/min ramp) for 4 h under N₂ flow. The yellow product was collected after cooling down furnace to room temperature.

B. Band gap and band positions calculation

The band gap was estimated on the basis of DRS spectra and Kubelka-Munk plot. The valence band (VB) and conduction band (CB) positions were calculated using the following equation.²

$$E_{CB} = \chi - E_e - \frac{1}{2} E_g \quad (1)$$

where E_{CB} is the CB position, E_e is the free energy of free electrons on the hydrogen scale (~4.5 eV), χ is the electronegativity of the semiconductor and E_g is the band gap of the semiconductor. Electronegativity is expressed as the geometric mean of the absolute electronegativity of the constituent atoms, and defined as the arithmetic mean of the atomic electron affinity and the first ionization energy. The calculated parameters for GCN and NS-CN are shown in Table S2.

C. Quantum efficiency calculation

The apparent quantum efficiency (AQE) was measured under the same photocatalytic reaction conditions. Four low-power 420 nm LED (3 W), which were positioned 1 cm away from the reactor in four different directions, were used as light source to trigger the photocatalytic reaction. The focused intensity for each 420 nm LED was ca. 6.0 mW/cm². AQE was calculated using equation 2. The AQE value obtained for NS-CN is ca. 1.71%.

$$AQE = \frac{2 \times \text{the number of evolved } H_2 \text{ molecules}}{\text{The number of incident photons}} \times 100\% \quad (2)$$

II. Supplementary Results

Table S1 Comparative interlayer spacing (d) and average crystal size (L) calculated from the powder XRD data using Brag's law and Scherrer's formula, respectively.

Photocatalyst	plane	d (nm)	L (nm)
GCN	(100)	0.648	1.38
	(002)	0.326	5.94
CN	(100)	0.639	1.30
	(002)	0.321	5.83
NS-CN	(100)	0.667	3.07
	(002)	0.328	3.84

Table S2 Energy band gap (E_g), valence band position (E_{VB}) and conduction band position (E_{CB}).

Photocatalyst	E_g (eV)	E_{VB} (V vs. NHE)	E_{CB} (V vs. NHE)
GCN	2.7	1.4	-1.3
NS-CN	2.5	1.62	-0.88

Table S3 Brunauer-Emmett-Teller (BET) surface area and Barret-Joyner-Halenda (BJH) pore size analysis data obtained for GCN and NS-CN.

Photocatalyst	S_{BET} ($m^2 g^{-1}$)	Pore volume ($cm^3 g^{-1}$)	Pore size (nm)
GCN	12	0.07	22.9
NS-CN	279	0.58	2.9

Table S4 A comparison of the hydrogen production rate obtained for NS-CN with the recently reported data for related photocatalysts.

Photocatalyst	H_2 production rate [$\mu mol h^{-1} g^{-1}$]	Ref.
GCN	106	1
GCN doped with C-dots	105	3
GCN	147	4
GCN (amorphous)	157.9	5
GCN (porous microsphere)	180	6
NS-CN	571.01	This work

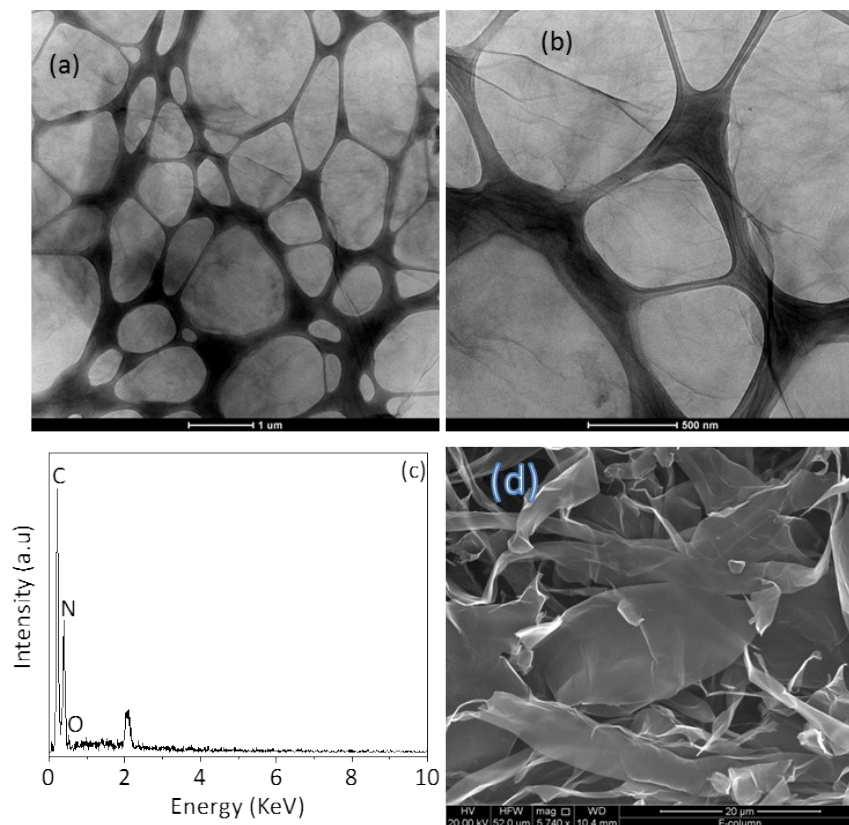


Fig. S1 (a-b) HRTEM images of NS-CN, (c) the corresponding EDX pattern and (d) SEM image of NS-CN.

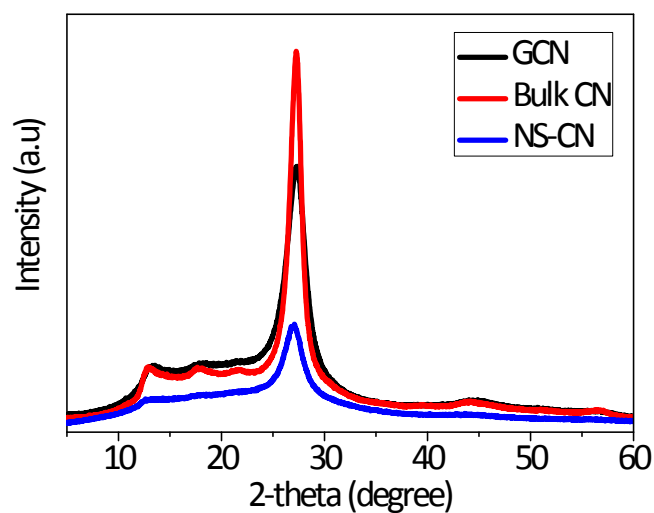


Fig. S2 The experimental XRD pattern recorded for NS-CN, bulk CN and GCN; the pattern obtained for NS-CN shows a sharp (002) diffraction peak at 27.1° and (100) diffraction peak at 13.27° , revealing a well-preserved graphitic structure. The peak at 27.1° represents the characteristic interlayer stacking structure of an aromatic

system. The peak at 13.27° indicates the interplanar structural packing and hole-hole distance of the nitride pores in the crystal.^{1, 7}

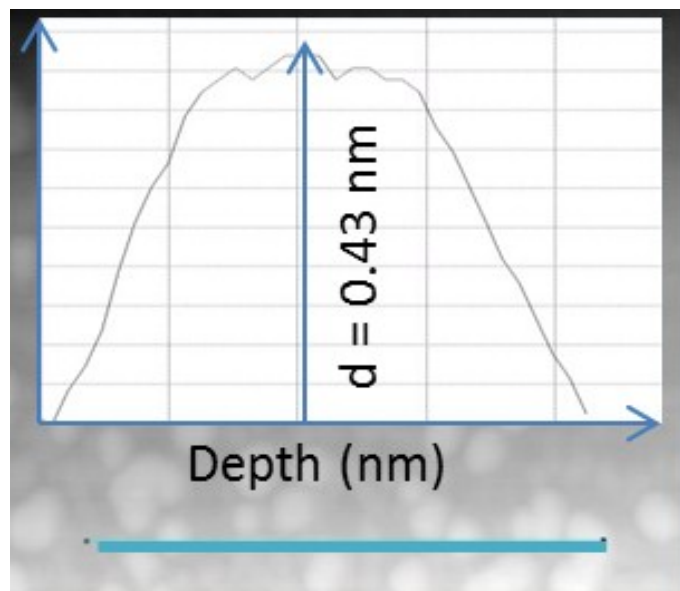


Fig. S3 Representative AFM image of NS-CN showing the corresponding thickness taken around the marked blue line.

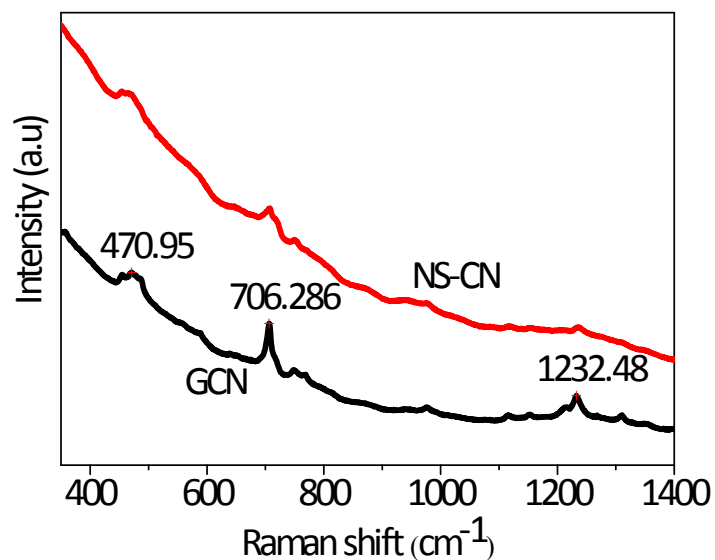


Fig. S4 Raman spectra (785 nm solid lasers) of NS-CN and GCN.

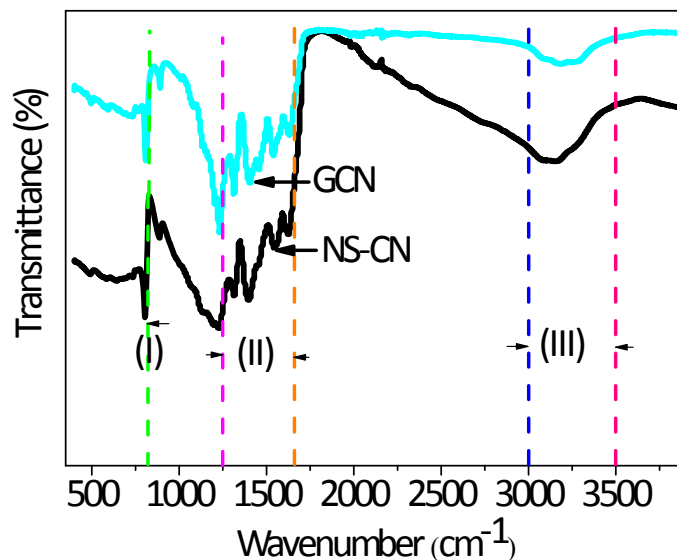


Fig. S5 Typical FTIR spectra consists of (i) breathing mode of tri-s-triazine units, (ii) stretching mode of aromatic CN heterocycles containing trigonal N(-C)₃ or bridging C-NH-C units, evidencing the formation of C-N-C bonds and (iii) stretching vibration of secondary and primary amines. The band at 809 cm⁻¹ on the FTIR spectrum is related to the triazine units of NS-CN nanosheets. The major bands between 1200 - 1650 cm⁻¹ represent the characteristic stretching modes of CN heterocycles, while the bands between 3000 - 3500 cm⁻¹ correspond to the stretching vibrations of -NH.³

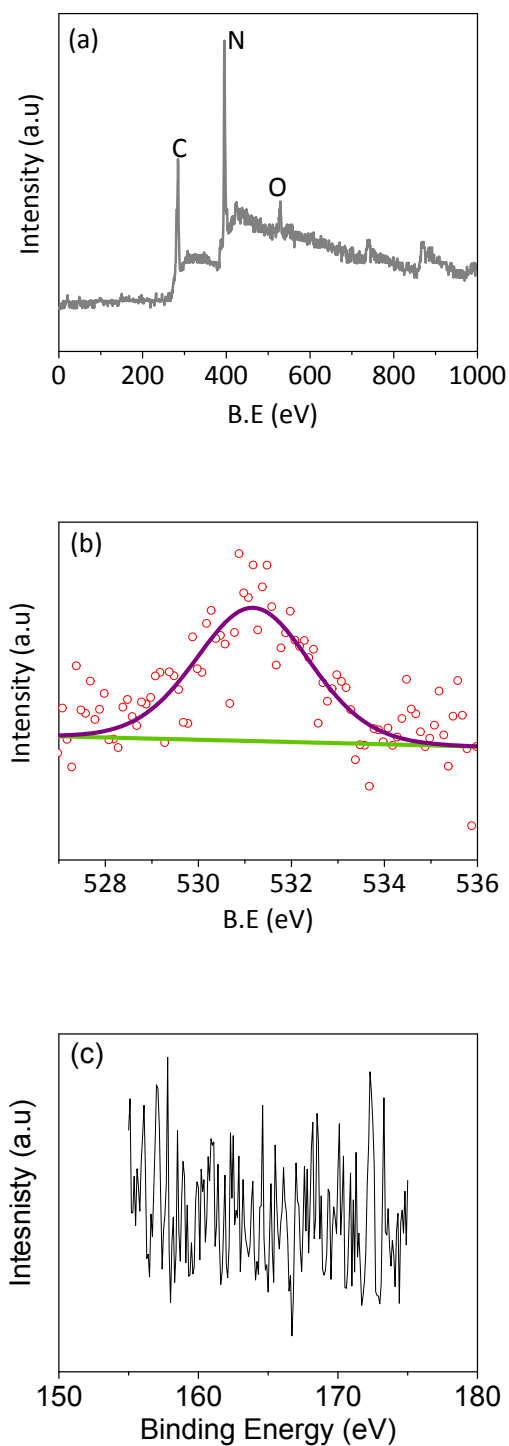


Fig. S6 XPS spectra of NS-CN. (a) Survey, (b) the O1s spectrum centred at 532.23 eV corresponding to O-C bonds in adsorbed oxygen species and (c) S2p spectrum.⁸

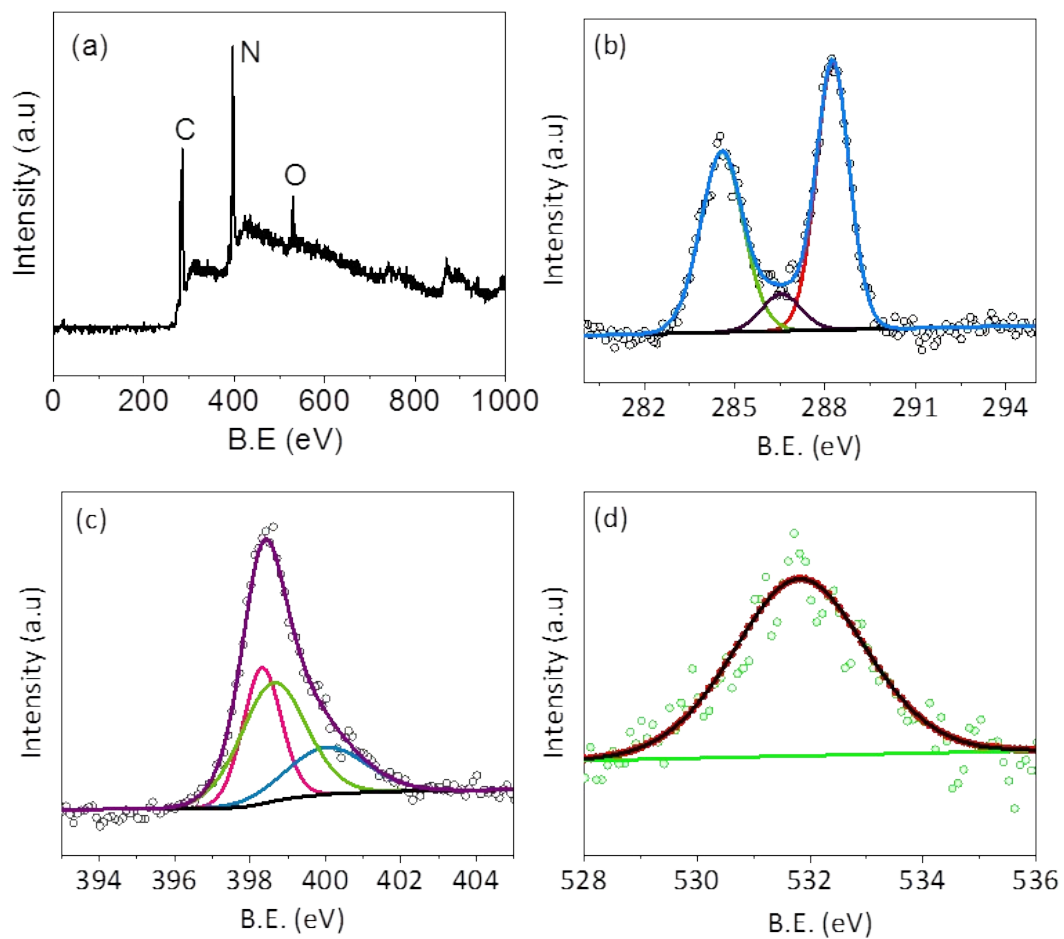


Fig. S7 XPS spectra of GCN. (a) Survey, (b) the deconvoluted C1s spectra, (c) the deconvoluted N1s spectra, and (d) the O1s spectrum.

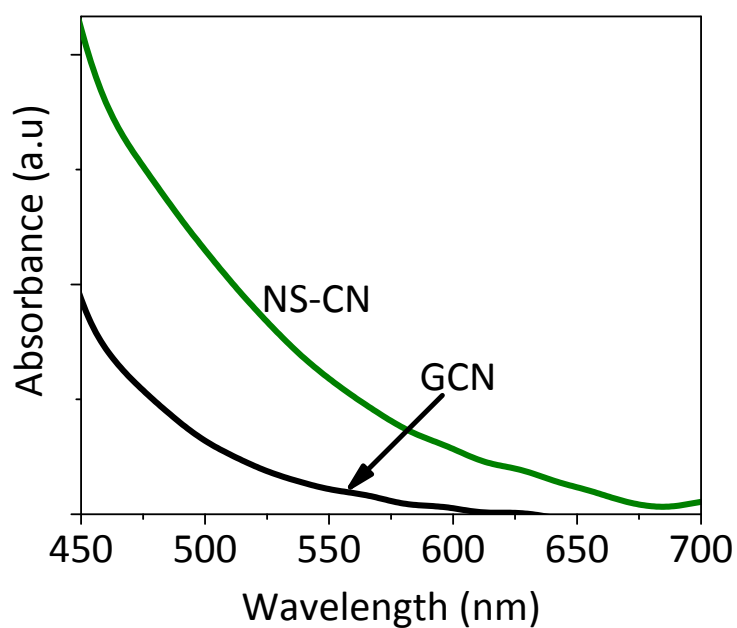


Fig. S8 UV-vis diffuse reflectance spectra of GCN and NS-CN for a selective range of photon wavelength (450 - 700 nm). In this selective range, photon absorption by graphitic carbon nitride obtained via traditional route is generally very poor, which has been shown as one of the main reasons for its low photocatalytic H₂ production rate via water splitting.⁸ However, NS-CN showed an enhanced photon absorption in the wavelengths range at 450 - 700 nm.

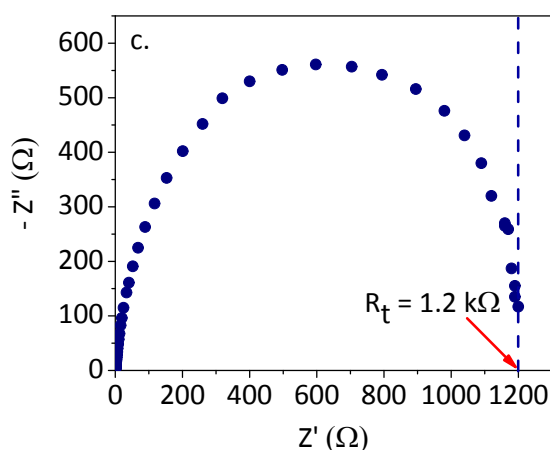
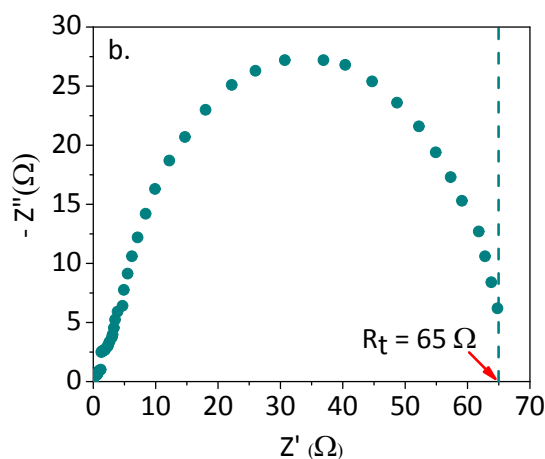
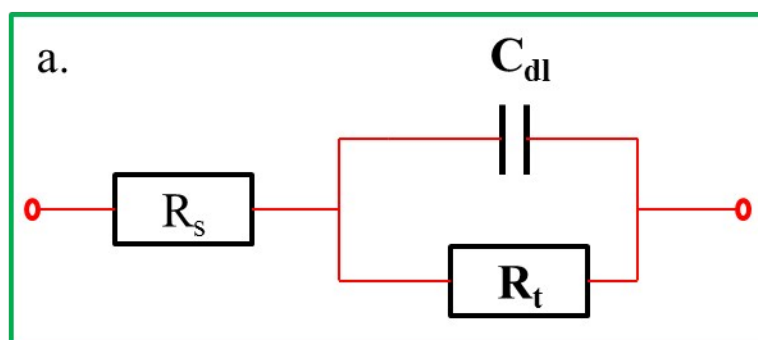


Fig. S9 (a) Equivalent electric circuit model for simulation of semicircle in the Nyquist plot. Here, the R_s is the electrolyte solution resistance, R_t is the charge-transfer resistance of the photocatalyst and C_{dl} is the double-layer capacitance. (b) Nyquist plot for NS-CN, where the red-arrow mark shows the approximate charge-transfer resistance, R_t (c) Nyquist plot for GCN. The red-arrow mark shows the approximate charge-transfer resistance, R_t which is over 18 times higher than that measured for NS-CN, indicating that the charge-transfer efficiency is significantly higher for NS-CN.

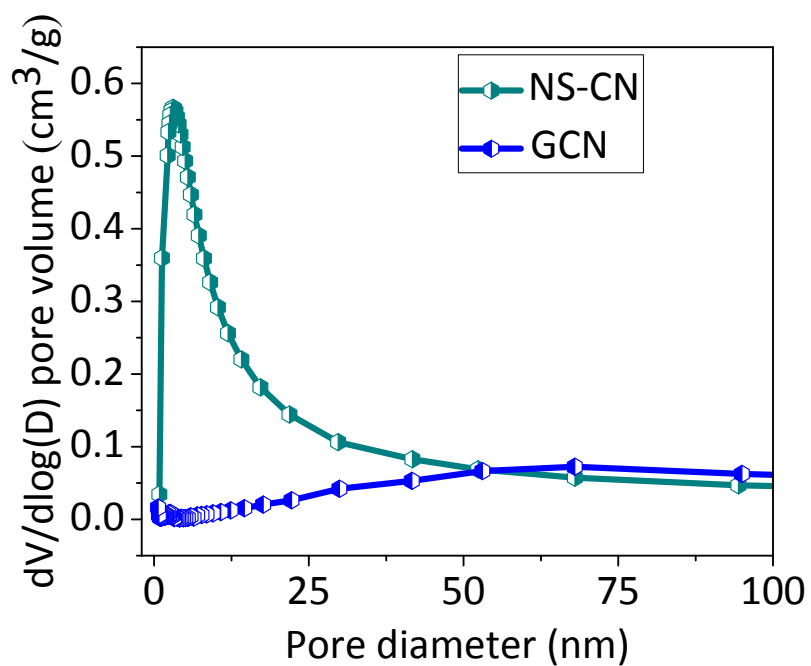


Fig. S10 Pore size distributions for both NS-CN and GCN.

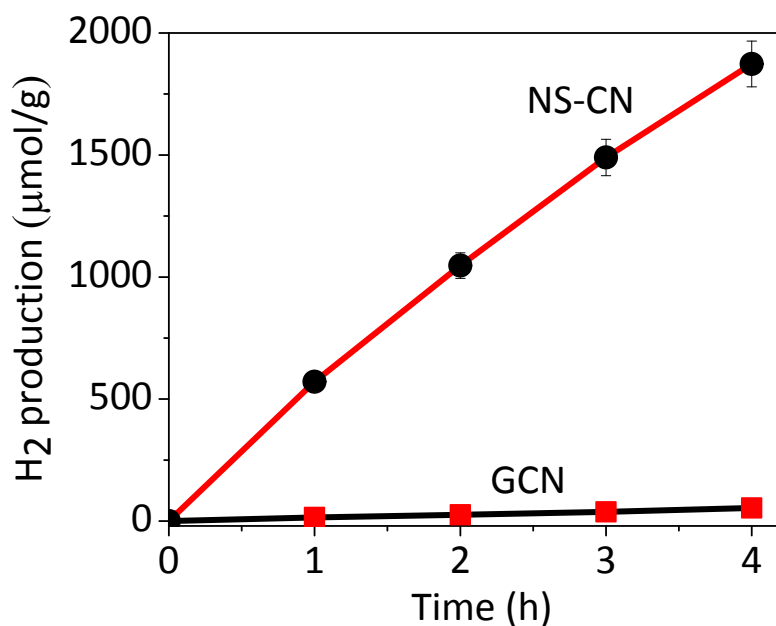


Fig. S11 A comparison of the hydrogen production rates obtained for pristine GCN and NS-CN using 10 vol% triethanolamine under visible light before first evacuation.

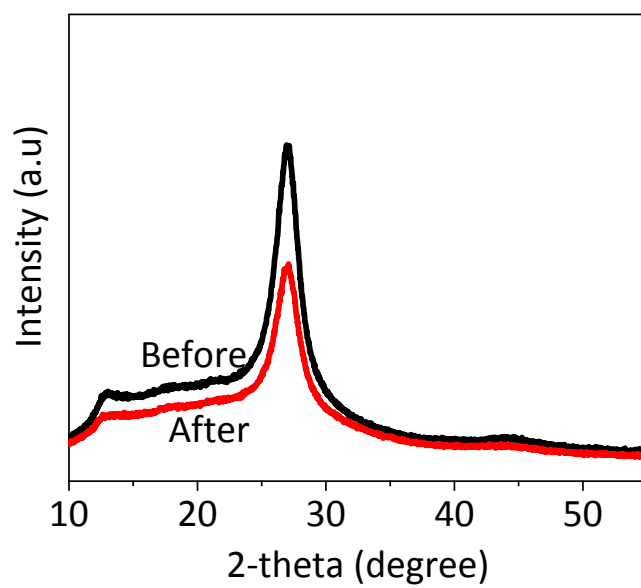
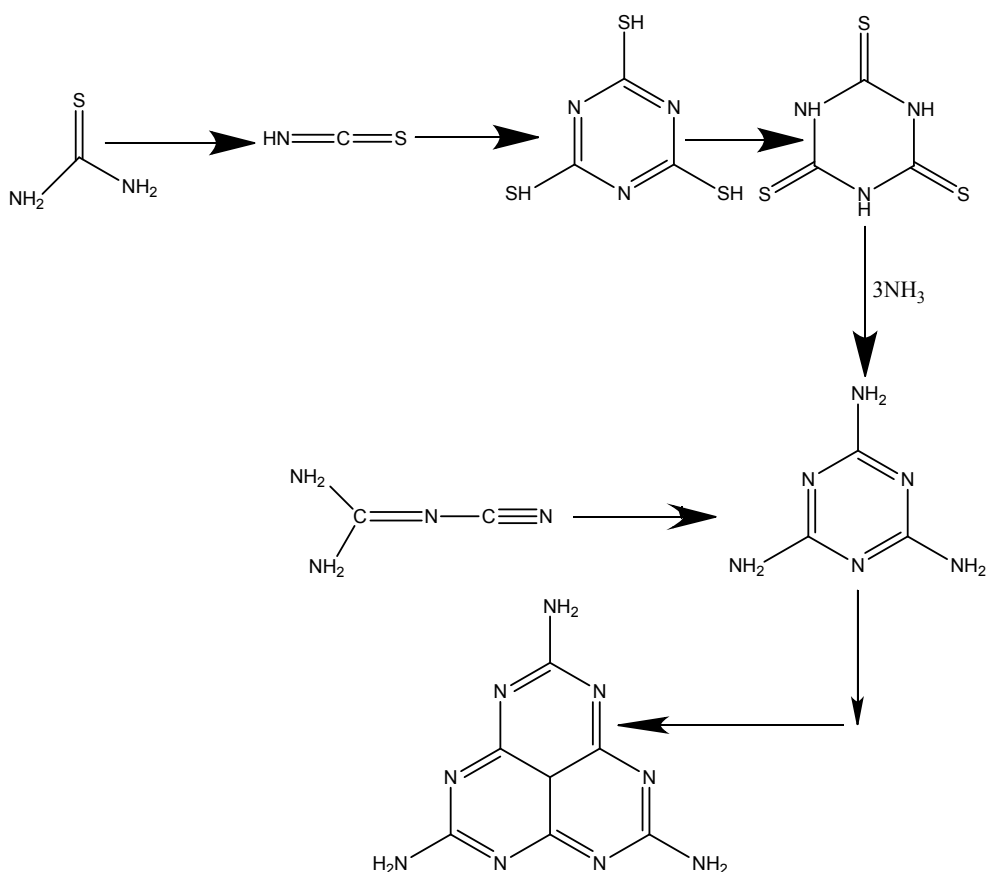


Fig. S12 (a) XRD patterns recorded for NS-CN before and after photocatalytic test.



Scheme S1 Possible reaction path for thiourea and DCDA polymerization leading to polymeric carbon nitride.

Dicyandiamide is thermally decomposed to melamine, whereas thiourea is decomposed to ammonia and isothiocyanic acid, which tend to form triple hydrogen bonded melamine-isothiocyanic complex. The isothiocyanic acid reacts with NH_3 to form melamine which is re-arranged to form covalent tri-s-triazine path. The polymerization continues via tri-s-triazine path and melamine is condensed to a melon chain by releasing of NH_3 . The pre-condensed melon chain is diffused through further elimination of significant amounts of ammonia to form the graphitic carbon nitride polymer.

References:

1. X. Wang, K. Maeda, A. Thomas, K. Takanabe, G. Xin, J. M. Carlsson, K. Domen and M. Antonietti, *Nat. Mater.*, 2009, 8, 76-80.
2. J. Ran, J. Zhang, J. Yu and S. Z. Qiao, *ChemSusChem*, 2014, 7, 3426-3434.
3. J. Liu, Y. Liu, N. Liu, Y. Han, X. Zhang, H. Huang, Y. Lifshitz, S.-T. Lee, J. Zhong and Z. Kang, *Science*, 2015, 347, 970-974.
4. Q. Xiang, J. Yu and M. Jaroniec, *J. Phys. Chem. C*, 2011, 115, 7355-7363.
5. Y. Kang, Y. Yang, L.-C. Yin, X. Kang, G. Liu and H.-M. Cheng, *Adv. Mater.*, 2015, 27, 4572-4577.
6. Q. Gu, Y. Liao, L. Yin, J. Long, X. Wang and C. Xue, *Appl. Catal., B*, 2015, 165, 503-510.
7. J. Zhang, X. Chen, K. Takanabe, K. Maeda, K. Domen, J. D. Epping, X. Fu, M. Antonietti and X. Wang, *Angew. Chem. Int. Ed.*, 2010, 49, 441-444.
8. A. Thomas, A. Fischer, F. Goettmann, M. Antonietti, J.-O. Muller, R. Schlögl and J. M. Carlsson, *J. of Mater. Chem.*, 2008, 18, 4893-4908.